

Tomur: Traffic-Aware Performance Prediction of On-NIC Network Functions with Multi-Resource Contention

Shaofeng Wu*
CUHK

Qiang Su*
CUHK

Zhixiong Niu
Microsoft Research

Hong Xu
CUHK

Abstract

Network function (NF) offloading on SmartNICs has been widely used in modern data centers, offering benefits in host resource saving and programmability. Co-running NFs on the same SmartNICs can cause performance interference due to onboard resource contention. Therefore, to meet performance SLAs while ensuring efficient resource management, operators need mechanisms to predict NF performance under such contention. However, existing solutions lack SmartNIC-specific knowledge and exhibit limited traffic awareness, leading to poor accuracy for on-NIC NFs. This paper proposes Tomur, a novel performance predictive system for on-NIC NFs. Tomur builds upon the key observation that co-located NFs contend for multiple resources, including onboard accelerators and the memory subsystem. It also facilitates traffic awareness according to the behaviors of individual resources to maintain accuracy as the external traffic attributes vary. Evaluation using BlueField-2 SmartNIC shows that Tomur improves the prediction accuracy by 78.8% and reduces SLA violations by 92.2% compared to state-of-the-art approaches, and enables new practical usecases.

1 Introduction

SmartNICs have been prevalent in modern data centers to deploy diverse network functions (NF) due to their benefits in programmability and host resource saving [32, 36, 37, 39, 41, 49, 50, 57]. They typically integrate heterogeneous onboard resources, such as SoC cores and domain-specific hardware accelerators, to cater to various NF demands. Moreover, vendors are developing increasingly resourceful NICs to meet evolving offloading needs [11, 13, 55]. To fully leverage these resources, it is common practice to co-locate multiple NFs on the same NIC [31, 36, 41, 53].

Unfortunately, sharing SmartNIC resources among co-located NFs may lead to contention and performance degradation, posing challenges in maintaining the SLAs. One potential solution is to implement stringent resource isolation

mechanisms on SmartNICs. Yet, previous work on this front requires specific NIC hardware architecture support and substantial rewriting of NF programs to accommodate new isolation abstractions [31], thus limiting their practical deployment. Consequently, developers still need extensive hand-tuning to ensure simultaneous SLA fulfillment for co-located NFs, which is time-consuming and error-prone [31, 35, 41].

Ideally, if operators can predict the performance drop an NF will suffer before actually co-running it with other NFs on the same NIC, they can make better placement decisions on existing infrastructure and NF implementations. To achieve this, we need a systematic *on-NIC* NF performance prediction framework, which entails two new challenges.

First, on-NIC NFs often utilize diverse onboard resources including memory and various hardware accelerators, making it common that contentions occur across heterogeneous resources. Prior work on NF performance prediction has primarily focused on memory subsystem contention as the sole source of performance interference for on-server NFs [28, 42, 44] only. We showcase that the state-of-the-art SLOMO [42] encounters high prediction errors when co-locating NFs contend for both memory and regex accelerator on a BlueField-2 SmartNIC, with $\sim 20\%$ in the median and $\sim 60\%$ in the worst case (§2.2). The community lacks a clear understanding of (1) the impact of contention on individual domain-specific accelerators and (2) the overall effect of multi-resource contention taken together on performance.

Second, NF performance is heavily influenced by traffic attributes such as flow counts and payload features, which changes dynamically for each NF. Current frameworks often either assume fixed traffic attributes [32, 49], or can only deal with a limited range of variations in these attributes (*e.g.*, 20% in flow counts in [42]).

In this paper, we propose **Tomur**, a new performance prediction framework that explicitly considers multi-resource contention and dynamic traffic attributes. Tomur conducts offline profiling of on-NIC NFs to collect their performance under diverse synthetic contention levels and traffic attributes. Leveraging these profiles, Tomur trains a contention-aware

*Shaofeng Wu and Qiang Su contributed equally.

Network Function	Description	Accelerator	T	Framework
FlowStats [42, 49]	Flow statistics with aging.	None	✓	Click
IPRouter [42, 49]	L3 packet routing program.	None	×	Click
IPTunnel [29]	L3 packet fragmentation tunnel.	None	✓	Click
NAT [34, 41, 49]	Network address translation for IPv4 based on MazonNAT.	None	✓	Click
FlowMonitor [41, 47]	Per-flow status and hardware payload scanning monitor.	regex	✓	Click
NIDS [41, 42]	Network intrusion prevention by hardware-based packet inspection.	regex	✓	Click
IPComp Gateway [2, 54]	Hardware-based payload scanning and compression.	regex, compression	✓	Click
ACL [17, 34]	Access control list based on DPDK ACL.	None	×	DPDK
FlowClassifier [17, 60]	Flow tracking using hash table.	None	✓	DPDK
FlowTracker [6]	Packet processing pipeline with hardware-offloaded flow tracking.	None	✓	DOCA
PacketFilter [6]	A hardware-based pattern matching and PacketFilter.	regex	✓	DOCA

Table 1: Typical NFs and accelerators they require from SmartNICs. Common resources (CPU, memory, and NIC subsystems) are not shown. **T** means that the NF performance heavily depends on the traffic attributes. The regex-based NFs use the same rule set from [8]. The last column indicates the programming framework we use to implement each NF.

model for each NF, which is then used to predict the NF’s performance before its deployment, facilitating placement and other management decisions. We build Tomur for SoC SmartNICs due to their ease of programmability (*e.g.*, DPDK and Click support), and tackle the above technical challenges by leveraging critical characteristics of on-NIC NFs.

Multi-resource contention modeling. Tomur’s key idea here is to independently model individual resource contention and integrate these per-resource models together. We identify hardware accelerators and memory subsystems as primary sources of contention for on-NIC NFs. For accelerators, we find that it is a common design for NFs to interact with them through their own queues which are then coordinated by simple round-robin scheduling. This inspires us to take a white-box approach and propose a queueing-based contention model for accelerators. Memory subsystem contention can be modeled using a black-box ensemble-based ML model following existing work [42]. Then, to capture the end-to-end effect of each resource contention, we introduce *execution-pattern-based composition*. This makes intuitive sense because how each resource and its contention affects the overall performance critically depends on the NF’s execution pattern, *e.g.*, pipeline or run-to-completion.

Traffic-aware modeling. On top of multi-resource contention, Tomur employs *traffic-aware augmentation* to integrate knowledge of traffic attributes into per-resource models. Generally speaking, this can be done by feeding *traffic attributes*, *e.g.*, flow count and packet size, as additional input features to per-resource models. Specifically, for accelerators, we can leverage the white-box nature of the queueing-based model and represent key model parameters as a function of traffic attributes; for memory subsystem which has a black-box model, we simply fuse traffic attributes with performance counters as the input feature to extend the model. In addition, to curb the high profiling cost caused by the introduction of traffic attributes especially for black-box memory models, Tomur adopts *adaptive profiling* to prune traffic attribute

dimensions and enforce targeted sampling at performance-critical ranges of the attributes.

We implement Tomur in C and Python, leveraging typical offline profiling tools [18–20, 22] and *sklearn* [21], and evaluate it on 9 common NFs using the popular BlueField-2 SmartNIC. Our code is open source anonymously at [14]. Our testbed evaluation shows that Tomur achieves accurate NF throughput predictions under multi-resource contention and varying traffic attributes, with an average error of 3.7% across NFs which corresponds to 78.8% accuracy improvement compared to state-of-the-art SLOMO. As new usecases, we also illustrate that in NF placement, Tomur can reduce SLA violations by 88.5% and 92.2% compared to the classical greedy-based approaches [41, 53] and SLOMO, and in performance diagnosis it can deliver higher accuracy in identifying bottlenecks for on-NIC NFs.

2 Background and Motivation

We start by presenting the brief background of network functions and their resource contention on SmartNICs, followed by the unique challenges of developing a contention-aware performance prediction framework which motivate our work.

2.1 Background

SmartNICs have been widely used to offload various network functions (NFs) in modern data centers, mainly for their benefits in host resource saving and energy efficiency [30, 36, 37, 41, 49, 53]. The NFs leverage the onboard domain-specific hardware accelerators to achieve high throughput and low latency [34, 41, 42, 49]. We showcase some typical NFs seen across prior work [34, 41, 42, 49] and the types of resources they need in Table 1. Here Flow Monitor, NIDS, and PacketFilter require the regex accelerator for packet inspection and payload scanning, and IPComp Gateway requires both the regex and compression accelerators.

Contention degrades performance Recently, co-running multiple NFs on the same SmartNIC has become more com-

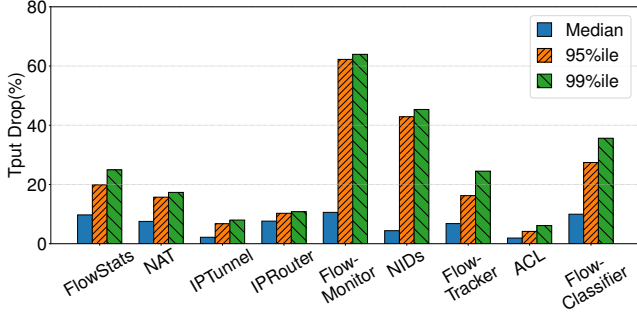


Figure 1: Throughput drop ratios of some NFs from Table 1 under resource contention when co-located with at most 3 other random NFs.

mon to improve utilization [31,36,41,53]. This can lead to performance degradation due to contention for shared resources. To demonstrate this effect, we profile the throughput drop of 9 typical NFs from Table 1 when they co-locate with other NFs. For each target NF, up to three other NFs are randomly selected (from Table 1).² Each NF is given two dedicated cores while sharing the memory subsystem and hardware accelerators due to the lack of hardware- or system-level isolation support on current SmartNICs. Traffic profiles for all NFs consisted of 16K flows of 1500B packets, with flow sizes following the uniform distribution (further details in §7.1). For NFs processing payloads with regular expressions, we use `exrex` [15] to generate packet payloads. Note the packet arrival rates are set sufficiently high for all NFs to ensure it is not causing throughput drop. We measure the throughput drop ratio against the baseline when the target NF runs alone with two CPU cores, the entire memory and hardware accelerators. Figure 1 depicts the statistics of throughput drop ratios. We can see that when co-running with different (numbers and combinations of) NFs, resource contention can cause 4.2% to 62.2% throughput drop at the 95%ile, and 1.9% to 10.6% at the median.

New challenges. Modeling and predicting NF performance under resource contention is therefore of paramount importance for many management tasks [28,32,42,44], and some prior work [28,42,44] has investigated this problem in network function virtualization where NFs run on commodity servers. An immediate question is, what makes contention-aware performance prediction different in the context of SmartNICs? We now highlight two unique challenges which are not well addressed in past efforts. Note all experiments in this section use the BlueField-2 (BF-2) SmartNIC.

2.2 Challenge 1: Multi-Resource Contention

We’ve seen that NFs on SmartNIC utilizes multiple heterogeneous onboard resources. Prior work, however, has only considered contention of the memory subsystems [28,42,44], missing the contention on other hardware accelerators. Their effectiveness as a result is tainted in the context of SmartNICs.

²Some NFs require minimum two cores, while one BlueField-2 has eight cores in total.

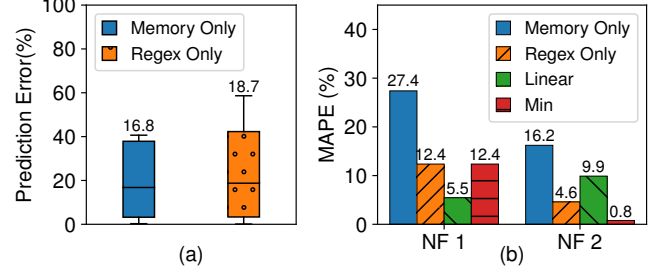


Figure 2: Prediction errors (absolute percentage error) of FlowMonitor’s throughput using single-resource models. (a) Box and whisker plot of using only the memory-based SLOMO model or a regex-based model (§4.1.1). We show the median error on top of each error box. (b) Mean average percentage error (MAPE) of sum and min composition of single-resource models. NF1 and NF2 adopt run-to-completion and pipeline resource usage pattern respectively.

To empirically substantiate our argument, we co-run FlowMonitor with up to three competing NFs chosen randomly from Table 1 on one BF-2. The traffic profiles are identical to the one in Figure 1. We use SLOMO [42] as the state-of-the-art memory-based prediction model and develop a new model for the regex accelerator due to lack of existing models (details in §4.1.1).

We first train our single-resource models for FlowMonitor which uses regex accelerator in addition to CPU and memory, and validate their effectiveness under single-resource contention. We build two synthetic NFs, *mem-bench* and *regex-bench*, to assert controllable memory and regex contention, respectively, for generating training data (details in §6). Following SLOMO, we also collect data from our BF-2’s performance counters at runtime (e.g., memory read/write rates) as the model input. Absolute percentage error against FlowMonitor’s true throughput under single-resource contention is used as the loss function. Our models achieve the same <10% average prediction error for memory- and regex-only contention as reported in the SLOMO paper [42] (Tables 11 and 12 in Appendix §A).

Then we apply these models directly to the multi-resource contention scenario as said before, where co-locating NFs as a whole contend for both memory and regex accelerator and nothing else. Figure 2(a) shows that prediction error now increases to ~20% in the median and reaches ~60% in the worst case, indicating that only considering one resource is wildly inaccurate.

In addition, NFs exhibit diverse execution patterns when utilizing these resources. For example, one NF may run in a *pipeline* manner for high throughput, while another may wait for the completion of dispatched requests to ensure low average latency (*run-to-completion*) [20,32]. This makes *composition* of single-resource models, a strawman solution for multi-resource prediction, inaccurate.

To explore this, we analyze two simple composition approaches: (1) *sum composition*, which adds up the predicted throughput loss from each model [32,59], and (2) *min composition*, which uses the minimal predicted throughput loss

as the final output [41, 52]. Figure 2(b) presents the results of these two approaches in the same setting as Figure 2(a). We observe that while composition models reduce error, they do not guarantee optimal accuracy across all NFs. For NF1 with run-to-completion, sum composition works better, but its error is significant ($\sim 17\%$) for the pipeline NF2. The key reason is that the resource contention impact on end-to-end throughput varies by NF execution patterns. In pipeline-based NFs, throughput is constrained by the slowest stage on which resource contention causes the most significant performance interference compared. In contrast, for run-to-completion NFs, contention on different resources uniformly impacts the end-to-end throughput.

To quickly recap, NFs on SmartNICs can experience contention across multiple resources, and its impact on performance differs according to the execution patterns. Current systems consider only single-resource contention, which results in substantial prediction inaccuracies.

2.3 Challenge 2: Traffic Attributes

An NF’s performance also depends on certain traffic attributes, such as number of flows, payload characteristics, etc., in many cases [32, 42, 49]. To see this, we measure FlowStat’s throughput when co-located with mem-bench, and vary mem-bench’s cache access rates (CAR). Figure 3(a) shows that FlowStat’s throughput drops differently in different traffic profiles as mem-bench’s CAR increases, implying that a traffic-agnostic model inevitably leads to high prediction errors when adapting to new traffic profiles.

Figure 3(b) empirically confirms the intuition above for existing work. Here we look at three target NFs: FlowStats, FlowClassifier, and FlowTracker. Each of them is co-located with mem-bench on a single BF-2. We use the same default traffic profiles of 16K flows to train three models for each target NF following SLOMO just as in the experiments before. We then test them under changing traffic attributes by generating 100 distinct traffic profiles with random number of flows up to 500K. It is clear from Figure 3(b) that prediction error increases dramatically when the traffic behavior deviates from the default profiles that the models have seen. Note SLOMO does consider the number of flows in its prediction, but can only handle a small degree of deviation from the training data as we shall detail in §7.1 and §7.4.

3 Tomur Overview

The challenges in §2 pose two fundamental questions on accurate performance prediction for on-NIC NFs, which drive Tomur’s design:

1. How to model the impact of multi-resource contention on NF performance?
2. How to integrate traffic attributes to contention-aware performance prediction models?

We develop Tomur, a framework for accurately predicting on-NIC NF performance with multi-resource contention and

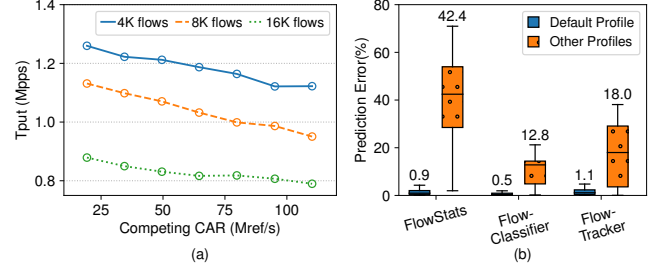


Figure 3: (a) FlowStats’s throughput when the competitor’s cache access rate (CAR) changes in three distinct traffic profiles. CAR is the sum of the cache read and write rates obtained from the hardware performance counters on BlueField-2. (b) Distribution of prediction errors after adapting the model to different traffic profiles. We show the median error on top of each error box.

varying traffic profiles. To address the first design question, Tomur adopts a “divide-and-compose” approach: it builds up individual *per-resource contention models* (§4.1) for both hardware accelerators and memory subsystem to separately model their impact on throughput, and applies *execution-pattern-based composition* (§4.2) to faithfully capture the end-to-end effect of contention. Then in response to the second design question, Tomur introduces *traffic-aware augmentation* (§5.1) techniques to integrate various traffic attributes into per-resource models, and develops an *adaptive profiling* (§5.2) method to balance the soaring profiling costs (due to the extra dimensions of traffic attributes) with model quality. Taken together, during online prediction, Tomur takes the contention level of competing NFs and traffic attributes of the target NF as input to the per-resource models and compose the results based on NF’s execution pattern to obtain the final prediction. Detailed workflow is in Appendix §F. Consistent with prior work [32, 42, 44], Tomur does not require knowledge of or access to NF source code.

4 Multi-Resource Contention Modeling

We now present the design insights and details of Tomur’s multi-resource contention modeling. Note we are interested in the NF’s maximum throughput assuming the arrival rate is high enough, which represents the NF’s capability and is consistent with prior work [42, 44].

4.1 Per-Resource Models

An on-NIC NF consumes onboard CPU, memory subsystem (cache and main memory), hardware accelerators, and NIC [31, 32, 35, 49]. For CPU, given common deployment practice [54, 56, 60], we perform core-level isolation for co-located NFs so CPU contention does not happen. Although some prior work has discussed potential isolation issues for NICs on a server [35], we do not encounter this problem as on-NIC NFs leverage powerful hardware-based flow table on SmartNICs [6]. Thus, we focus on contention on hardware accelerators and memory subsystem here, assuming fixed traffic attributes. Notice the per-resource modeling effectively derives the NF’s throughput on one given resource only without accounting for other resources, and may not equal to the overall throughput.

4.1.1 Hardware Accelerators

At first glance, modeling hardware accelerator contention seems not much different from existing design for memory contention [42, 44]. That is, one can use an accelerator’s performance counters to quantify NF’s contention level as the input, and employ an ML model to predict throughput. This is infeasible, however, because current SmartNIC accelerators do not expose fine-grained performance counters [3, 10, 12, 19, 39]. We thus propose a general *queue-based* white-box approach for hardware accelerators.

Contention behavior in hardware accelerators. We start by analyzing the accelerator’s contention behavior which our modeling is based upon. Without loss of generality, we use the widely-used regex accelerator [6, 12, 20] as the target of discussion hereafter.

In practice, NFs utilize onboard accelerators via the corresponding queue systems [6, 7]. For example, an NF establishes request queues and enqueues/dequeues operations to/from a regex accelerator [6, 7, 20]. This queue-based interface unifies the interaction with specialized accelerators and applies to many SmartNICs [10, 11, 13] and beyond [1, 33]. Understanding the queue system behavior is then crucial for modeling accelerator contention.

Setup. We write a synthetic Click NF called regex-NF that utilizes regex accelerator to scan packet payloads. regex-NF’s packet arrival rate is high enough to ensure maximum throughput, and it is tested with different match-to-byte ratios (MTBR).³ To vary contention level, we adjust the co-running regex-bench’s arrival rate.

Observation. We depict the throughput results in Figure 4 and make two interesting observations. *O1*: First, regex-NF shows *linear* throughput drop as the contention from regex-bench rises. *O2*: Second, regex-NF finally reaches the equilibrium throughput without further dropping. The equilibrium point clearly varies with regex-bench’s MTBR.

These two observations are very familiar to us as they point to the canonical round-robin (RR) queuing discipline widely used in practice. Indeed, we confirm from [9] that our regex accelerator driver’s implementation adopts RR for queue-level fairness. With one queue per each NF which is the setup in our experiment, as regex-bench’s request arrival rate increases, regex-NF’s requests have proportionally less access to the accelerator, resulting in the linear throughput decline. When contention is high enough that regex-bench’s queue is always non-empty when the RR scheduler turns to it, throughput of regex-NF stops dropping since its average sojourn time (sum of queueing and processing times) stops increasing [46]. As they have the same numbers of queues, their equilibrium throughput is the same as seen in Figure 4.

Our approach. Motivated by the above analysis, the regex

³Match-to-byte-ratio (MTBR) refers to how many matches against a regex ruleset is contained in each byte of the payload. A higher MTBR reflects more regex matches with in each unit of packet payload and longer processing time for a packet (§7.1).

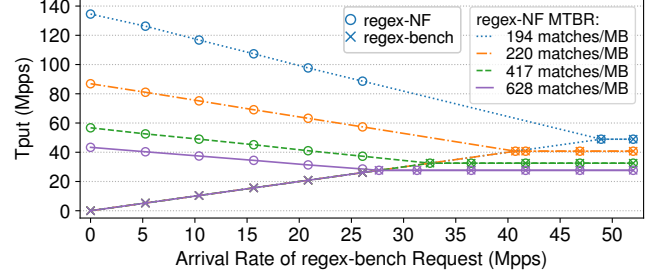


Figure 4: Throughput of co-running synthetic pattern-matching “regex-NF” and regex-bench as a function of arrival rate of regex-bench. The packet size is 1500B. In each setting, regex-NF and regex-bench reach an equilibrium throughput, *e.g.*, with MTBR of 194 matches/MB for regex-NF, they both obtain 48.9 Mpps at equilibrium.

accelerator contention can be modeled by RR over multiple request queues with one service node (*i.e.*, the accelerator). Suppose we have N NFs sharing an accelerator, and each NF_j has n_j request queues. At equilibrium, the average sojourn time t of requests from each queue is [46]:

$$t = \sum_{j=1}^N n_j t_j, \quad (1)$$

where t_j represents NF_j ’s average request processing time. For a target NF_i , its throughput T_i can be represented as the sum of throughput of all its queues, *i.e.*,

$$T_i = \frac{n_i}{t} = \frac{n_i}{\sum_{j=1}^N n_j t_j} = \frac{n_i}{\sum_{j=1}^N \frac{n_j^2}{T_{j,solo}}}, \quad (2)$$

where $T_{j,solo}$ represents its regex processing throughput (in pps) when NF_j runs solo. Clearly when $n_i = n$ for all NFs, they have the same (equilibrium) throughput T_i .

Now to use Equation (2) for a new NF, we need to infer n_j and $T_{j,solo}$ without any knowledge of the NF. Recall $T_{j,solo}$ is throughput on the regex accelerator only, which may or may not equal to end-to-end throughput if the NF is bottlenecked on other resources or follows run-to-completion. So to estimate them accurately, we again co-run the NF with regex-bench and set regex-bench’s request processing time and match rate to be high enough to ensure that at equilibrium, the NF spends most of its time on regex. We then collect two sets of equilibrium throughput data to solve for n_j and $T_{j,solo}$ since regex-bench’s parameters are known.

We leverage Equation (2) to derive the equilibrium throughput under two one-queue NFs (Appendix §E) just as in Figure 4, and verify with empirical results of various regex-based NFs (Appendix §A) that our approach is accurate with 1.3% error on average.

Other accelerators. Our approach here directly applies to other hardware accelerators, *e.g.*, compression and crypto accelerator, which also uses round-robin based queues [9, 17].

4.1.2 Memory Subsystem

Memory subsystem contention has been studied in existing work [28, 42, 44] which finds that the contention-induced throughput drop can be modeled as a *piece-wise linear* function of performance counters (Figure 9 in Appendix §B). Thus we follow SLOMO’s gradient boosting regression (GBR) method which is state-of-the-art, using 7 performance counters (Table 13 in Appendix §D) as input features. Note that we overcome the fixed-traffic limitation of GBR by integrating traffic attributes to it in §5.

4.2 Execution-Pattern-Based Composition

We now discuss how to composite the per-resource models for deriving end-to-end throughput.

Observations. We analyze two typical execution patterns of NFs: *pipeline* and *run-to-completion* [20, 32]. Considering a packet received by a pipeline NF, or p-NF, and a run-to-completion NF, or r-NF: for p-NF, the packet waits at the first stage until its predecessor *enters* the second stage; for r-NF, the packet waits until the predecessor *leaves* the last stage.

Figure 5 presents the throughput of a synthetic p-NF (top) and r-NF (bottom) under different levels of memory and regex accelerator contention. We observe that: *O1*: the p-NF’s throughput stays unchanged when memory contention is low and regex contention is high. For example, the throughput stays at ~ 400 Kpps when competing cache access rate (CAR) is less than ~ 100 Mref/s and competing match rate (product of throughput and MTBR) is 2500 Kmatches/s. This is because the throughput of a pipeline equals that of its slowest stage — regex matching in this case, making it insensitive to memory subsystem contention. *O2*: Second, for the r-NF, we observe that throughput drop is a *monotonically decreasing* function of both competing CAR and regex match rate, indicating that throughput drop is always caused by the compounded contention.

Our approach. The main goal here is to derive a composing function that takes in execution pattern and per-resource throughput drop ΔT_k , $1 \leq k \leq r$ (given by per-resource models) as input, and produces the end-to-end throughput drop caused by contention in r resources.

Pipeline: Based on *O1*, end-to-end throughput (denoted as T) of a p-NF can be calculated as:

$$T = T_{solo} - \max(\Delta T_1, \dots, \Delta T_r), \quad (3)$$

where T_{solo} is the NF’s throughput when running solo.

Run-to-completion: Based on *O2*, we denote the processing time of a packet in each resource without contention as t_k (also the sojourn time), where $1 \leq k \leq r$. Due to multi-resource contention, the sojourn time of a packet in each resource grows by Δt_k as a result of throughput drop ΔT_k . Therefore, the throughput of the r-NF can be represented as:

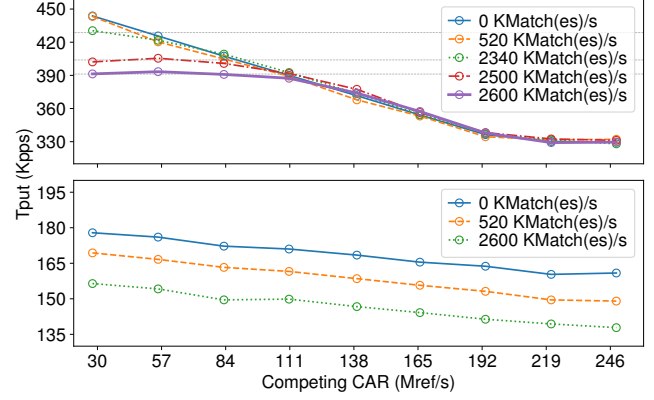


Figure 5: Throughput of two synthetic Click NFs that use pipeline (top) and run-to-completion (bottom) as a function of competing CAR in memory subsystem and match rate in regex accelerator.

$$\begin{aligned} T &= \frac{1}{\sum_{k=1}^r (t_k + \Delta t_k)} \\ &= \frac{1}{\sum_{j=1}^r \left(t_j + \Delta t_j + \sum_{k=1, k \neq j}^r t_k \right) - \sum_{j=1}^r \sum_{k=1, k \neq j}^r t_k} \quad (4) \\ &= \frac{1}{\sum_{j=1}^r \frac{1}{T_{solo} - \Delta T_j} - \frac{r-1}{T_{solo}}} \end{aligned}$$

Detecting execution pattern. Without source code access, we resort to a simple testing procedure to detect an NF’s execution pattern. We co-run the NF with our benchmark NFs, and see if Equation 3 or 4 fits its throughput drop better. One may also observe the NF’s throughput curve similar to Figure 5 to empirically determine if it is a p- or r-NF.

5 Traffic-Aware Prediction

Our discussion so far has been limited to fixed NF traffic profiles. Now we discuss how to integrate traffic attributes into our models.

5.1 Traffic-Aware Augmentation

It is obvious that we need to augment the per-resource model with knowledge of traffic attributes, while execution-pattern-based composition is not affected. To do this, we select three common traffic attributes that impact NF performance based on our experiment results and previous studies [32, 42]: number of flows or flow count, packet size, and match-to-byte-ratio (MTBR) of a packet. We denote a traffic profile of 16K flows, 1500B packets and 600 matches/MB payload using a vector (16000, 1500, 600).

5.1.1 Hardware Accelerators

We again start with hardware accelerators, specifically the regex accelerator, as a concrete example.

Our approach. A regex-utilizing NF is naturally sensitive

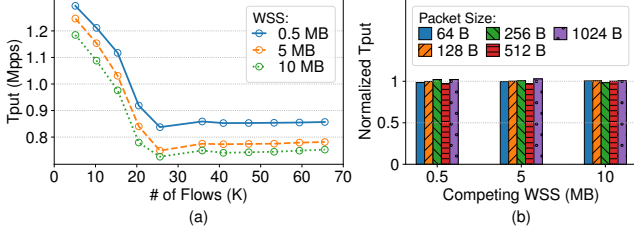


Figure 6: Throughput of FlowStats as a function of traffic attributes. (a) The packet size is 1500 B. (b) The number of flows is 16 K.

to the MTBR of packet payload [20].⁴ It directly impacts the average processing time of the regex requests.

Following notations from Equation 2, the average request processing time of NF_j for a given ruleset can be expressed as:

$$t_j = \frac{1}{T_{j,solo}} = t_{j,0} + a_j m_j, \quad (5)$$

where $t_{j,0}$ and a_j are constants, and m_j is the MTBR. Equation 5 builds on the intuition that that request processing time grows linearly with number of matches in a packet, as each match induces a constant amount of extra processing time on average on top of the base processing time. Plugging into Equation 2, the traffic-aware throughput model of regex accelerator is:

$$T_i = \frac{n_i}{\sum_{j=1}^N n_j^2 (t_{j,0} + a_j m_j)}. \quad (6)$$

The parameters $t_{j,0}$, a_j can be easily obtained from linear regression using data from co-running the NF with regex-bench under different MTBRs.

Other accelerators. Per-resource models for other accelerators can be augmented in a similar two-step approach: (1) analyzing what accelerator-specific traffic attributes affect the NF; (2) representing the average processing time as a function of these accelerator-specific traffic attributes.

5.1.2 Memory Subsystem

Observation. We co-run FlowStats with mem-bench with different numbers of flows (other traffic attributes stay the same). We adjust the working set size of mem-bench and keep other metrics (*i.e.*, CAR and memory access rate) fixed. Figure 6(a) reveals that FlowStats experiences significant throughput drop with increasing flow count. More interestingly, the throughput curve is also a *piece-wise* function of the number of flows, which is similar to memory contention modeling as mentioned in §4.1.2.

Our approach. Thus, we take a straight-forward approach to add traffic attribute knowledge as extra features to the black-box GBR model of memory subsystem, by appending the traffic attributes vector to the original input vector of performance counters.

⁴Number of queues is fixed during NF’s life cycle per its configuration.

5.2 Adaptive Profiling

Being traffic-aware brings a new and critical issue: training a traffic-aware model now needs more data due to the higher dimensionality of the input vector compared to a fixed-traffic model. This is especially true for the black-box model for memory subsystem, which already has a high-dimensional input vector. A naive solution is to repeat the collection process for each unique traffic profile (*a.k.a.* full profiling), which obviously leads to massive exponentially-growing profiling overheads. Although random sampling based profiling [42, 44] can effectively reduce overhead, it may cause high prediction error due to inadequate coverage of the data space. The trade-off between profiling cost and model accuracy motivates us to design an optimized profiling method for Tomur.

Observations. Our design has roots on two key observations. First, an NF’s performance is only dependent on a few traffic attributes. For example, FlowStats is only sensitive to number of flows as in Figure 6(a), but not packet size as in Figure 6(b), since it only processes packet header information.

Second, for a given traffic attribute, it causes significant performance drops only in a limited range of values; performance shows little changes in other ranges. Still using FlowStats, when the competing WSS is 10MB, its throughput loses $\sim 30\%$ for $[1, 20K]$ flows, but remains almost unchanged for $[40, 60K]$ flows as in Figure 6(a). This is because FlowStats’s hash table grows as a result of growing flow count. Before it fully occupies the last level cache (LLC), increasing the hash table size leads to higher cache miss ratio, which slows down read/write operations and thus throughput. After the LLC is saturated, cache miss ratio stays at a fixed level, causing NFs to exhibit constant throughput. These characteristics also hold in general across NFs as we empirically observe for other NFs in Table 1. This is because generally, (1) NFs typically process either packet headers or payloads, which only depends on several traffic attributes; and (2) traffic attributes usually affect performance by changing the size of key data structures in the NF processing logic, *e.g.*, the mapping table in NAT [29, 42, 44], which exhibits the same LLC effect as explained just now.

Our approach. Our key idea is to prune irrelevant traffic attribute dimensions, and conduct more sampling for relevant traffic attributes within the critical value ranges where NF performance has salient changes. We propose a two-step adaptive profiling algorithm that balances between model accuracy and profiling cost.

As shown in Algorithm 1, we first test whether NF performance is sensitive to a traffic attribute or not. Suppose the possible range of an attribute f is $[f_{min}, f_{max}]$. We profile the NF’s solo throughput using with f set to f_{min} and f_{max} respectively while other attributes remain default (lines 8-9). Then we compare the throughput difference to determine if f should be added in our model. Note that the function `profile_one()` collects throughput data under a specified

Algorithm 1 Adaptive profiling.

```
1:  $NF$ : The target NF to be profiled
2:  $C$ : The list of performance counters
3:  $F$ : The list of traffic attributes
4:  $Q, \epsilon_0, \epsilon_1, m$  are hyperparameters
5: function ADAPTIVE_PROFILE( $NF, C, F$ )
6:    $n \leftarrow 0$ 
7:   for  $f$  in  $F$  do
8:      $T_{min} \leftarrow \text{profile\_one}(NF, 0, f_{min}, n) \triangleright$  "0" represents no contention.
9:      $T_{max} \leftarrow \text{profile\_one}(NF, 0, f_{max}, n)$ 
10:    if  $|T_{max} - T_{min}| < \epsilon_0$  then
11:       $F \leftarrow F - f \triangleright$  Prune the traffic attribute dimension.
12:    RANGE_PROFILE( $NF, F_{min}, F_{max}, n$ )
13:  function RANGE_PROFILE( $NF, F_{min}, F_{max}, n$ )
14:     $T_{min} \leftarrow \text{profile\_one}(NF, 0, F_{min}, n)$ 
15:     $T_{max} \leftarrow \text{profile\_one}(NF, 0, F_{max}, n)$ 
16:    if  $n \geq Q$  then  $\triangleright$  We reach profiling quota
17:      return
18:    if  $|T_{max} - T_{min}| \geq \epsilon_1$  then  $\triangleright$  Only enforce collection when throughput changes drastically.
19:       $F_{mid} \leftarrow \frac{F_{max} + F_{min}}{2}$ 
20:      for  $_$  in  $m$  do
21:         $C_r \leftarrow \text{random}() \triangleright$  Contention level is random.
22:         $\text{profile\_one}(NF, C_r, F_{mid}, n)$ 
23:        RANGE_PROFILE( $NF, F_{mid}, F_{max}, n$ )
24:        RANGE_PROFILE( $NF, F_{min}, F_{mid}, n$ )
25:    return
```

configuration (contention level and traffic attribute), and increments the total number of collected samples by one if the configuration has not been profiled. After pruning the attribute list, we carry out a binary search to adaptively collect profiling data. For each call to `RANGE_PROFILE()`, we consider the difference between solo throughputs on traffic attribute boundaries. If their difference exceeds a certain threshold, we collect m data points at the center of current traffic attribute region (lines 18-22). Then the traffic attribute region is split in half, which will serve as the new region for the recursive call of `RANGE_PROFILE()`.

6 Implementation

We implement Tomur with ~ 1600 LoCs in C and Python. Tomur employs `perf-tools` [19] to collect performance counters (appendix §D). Tomur uses `sklearn` [21] to construct machine learning models used in per-resource models. Our code is open source anonymously at [14].

Synthetic benchmarking NFs. We implement three synthetic NFs called `mem-bench`, `regex-bench` and `compression-bench` (~ 8300 LoCs in C with DPDK support) based on open-source benchmark tools [7, 18, 20, 22] to apply configurable levels of contention on memory subsystem, regex, and compression accelerators, respectively. The `mem-bench` accesses an array

the system memory by varying: (1) access pattern, *i.e.*, stream access or step access, (2) access speed, and (3) the size of the array. `regex-bench` can adjust its processing rate and input profiles to induce different request rates and per-request Match-to-Byte Ratios (MTBR). Similarly `compression-bench` also varies its processing rate to induce different request rates and contention on the compression accelerator.

Network functions. We implement common on-NIC NFs with ~ 3600 LoCs in C and Click using frameworks including Click 2.1 [29], DPDK 20.11.6 [17], and DOCA 1.5-LTS [6]. Our BF-2 enables hardware flow table offloading for NFs. We present how we use these NFs to evaluate Tomur in §7.1.

7 Evaluation

We present our evaluation of Tomur now. The highlights are:

- (1) **Accuracy:** Tomur achieves an average prediction error of 3.7% end-to-end, with 78.8% error reduction compared to state-of-the-art across NFs (§7.2). Microbenchmarks further show that Tomur’s design choices on multi-resource contentions and changing traffic attributes are effective (§7.3, §7.4).
- (2) **Usecases:** To see how Tomur can be beneficial in practice, we show two concrete usecases where it (1) facilitates resource-efficient placement decisions in NF scheduling, reducing NF SLA violations by 88.5% and 92.2% compared to the classical greedy-based approaches and SLOMO, and (2) enables fast performance diagnosis for NFs under contentions with 100% accuracy (§7.5).
- (3) **Overhead:** Tomur’s offline adaptive profiling reduces profiling cost while maintaining high model accuracy, and takes less than 1 hour for each NF (§7.6).

7.1 Methodology

We employ NVIDIA BlueField-2 (BF-2) to evaluate Tomur. A BF-2 SmartNIC has 8 ARMv8 A72 cores at 2.5GHz, 6MB L3 cache, 16GB DDR4 DRAM, dual ConnectX-6 100GbE ports, and hardware accelerators for regex and compression. The NF traffic is generated from a client machine with an AMD EPYC-7542 CPU with 32 cores at 2.9GHz and a ConnectX-6 100GbE NIC. Both the BF-2 server and client machine are connected to a Mellanox SN2700 switch. Simultaneous multi-threading and turbo boost are disabled.

Traffic profiles. We employ `DPDK-Pktgen` [23] to create various traffic profiles with different attributes, *i.e.*, number of flows and packet sizes. The flow sizes follow a uniform distribution. In addition, we generate packet payloads using `exrex` [15] with diverse MTBR of conducting regular expression matches, *e.g.*, 600 matches/MB, for NFs using regex accelerator. The rule sets are from [8].

Training. We generate various traffic profiles as said above and collect NF’s performance to prepare training data. The default profile has 16K flows, 1500B packet size, and the MTBR at 600 matches/MB. To account for multi-resource

NF	SLOMO			Tomur		
	MAPE (%)	$\pm 5\%$ Acc.(%)	$\pm 10\%$ Acc.(%)	MAPE (%)	$\pm 5\%$ Acc.(%)	$\pm 10\%$ Acc.(%)
ACL	1.3	100.0	100.0	1.2	100.0	100.0
NIDS	16.2	24.3	74.3	1.5	95.9	100.0
IP Tunnel	62.9	70.5	73.1	3.8	75.6	92.3
IP Router	4.2	68.4	98.2	3.8	66.7	100.0
FlowClassifier	7.5	28.1	73.7	3.8	63.2	100.0
FlowTracker	4.9	56.1	86.0	3.9	61.4	100.0
FlowStats	11.7	33.3	57.9	4.3	70.2	96.5
FlowMonitor	40.9	31.1	41.9	4.5	62.2	93.2
NAT	8.2	38.6	49.1	6.4	42.1	80.7

Table 2: Prediction accuracy comparison under both multi-resource contention and varying traffic attributes. On average Tomur reduces MAPE by 78.8% compared to SLOMO, at 3.7% and 17.5%, respectively. Unless otherwise stated, rows of table are sorted in ascending order of Tomur’s MAPE.

contention, we rely on the three synthetic benchmark NFs in §6 to generate training data in different contention levels. Unless otherwise stated, we train three models for each NF using different random seeds, and all prediction results are averaged by all three models for numerical stability.

Baseline. SLOMO [42] serves as our baseline. For each NF, we train a model using SLOMO’s gradient boost regression under the default traffic profile (Table 13, Appendix §D). If in testing the traffic profile deviates from default, we employ SLOMO’s sensitivity extrapolation⁵ to adapt the model (Section 6 in [42]). We validate that our models achieve the same level of prediction error as in [42] (Appendix §A).

Metrics. We use the mean absolute percentage error (MAPE) commonly used in existing work [25, 42, 44] as the main metric of prediction accuracy. The ground truth is the NF’s real average throughput measured in identical deployment setup. To avoid the impact of test set size variations, we also report the number of prediction results experiencing errors within $\pm 5\%$ and $\pm 10\%$, and marked its percentage by the test set size as $\pm 5\%$ Acc. and $\pm 10\%$ Acc., respectively [59]. A larger value indicates higher accuracy.

NF. NF implementation details are given in §6. Each NF is allocated two dedicated CPU cores. Co-located NFs share the memory subsystem and hardware accelerators [4, 5, 41, 56, 60]. We always set traffic arrival rates (packets per second) high enough for NFs to achieve their maximum throughput.

7.2 Overall Accuracy

We first evaluate the overall prediction accuracy of Tomur under multi-resource contention and varying traffic attributes. Each target NF is co-located with up to three other NFs and we numerate all possible combinations of NFs. We also apply 9 distinct traffic profiles for each NF. The results are aggregated under all traffic profiles, as shown in Table 2. We can see that Tomur averagely exhibits 3.7% MAPE, 70.8% $\pm 5\%$

⁵“Sensitivity” refers to NF performance as a function of contention level for simplicity [28, 42–44].

NF	SLOMO			Tomur		
	MAPE (%)	$\pm 5\%$ Acc.(%)	$\pm 10\%$ Acc.(%)	MAPE (%)	$\pm 5\%$ Acc.(%)	$\pm 10\%$ Acc.(%)
NIDS	21.4	60.0	71.2	4.3	55.6	95.6
FlowMonitor	49.3	18.5	33.3	5.1	59.3	88.9

Table 3: Prediction accuracy of SLOMO and Tomur when the NF runs under only multi-resource contention. Traffic profile is fixed to the default one.

Acc. and 95.9% $\pm 10\%$ Acc., compared to SLOMO’s 17.5% MAPE, 50.0% $\pm 5\%$ Acc. and 72.7% $\pm 10\%$ Acc., demonstrating Tomur’s superior prediction accuracy. Specifically, Tomur has the most significant gains for IPTunnel, FlowMonitor, FlowStats, and NIDS that use multiple resources and/or is sensitive to traffic attributes. Meanwhile, Tomur achieves the same accuracy as SLOMO for ACL because it is very lightweight and insensitive to traffic attributes. Note that the high prediction accuracy for such NFs is aligned with that from previous studies [28, 42, 44].

Next, we microbenchmark Tomur’s major design choices to better understand the benefits they each bring.

7.3 Deep-Dive: Multi-Resource Contention

First we look at how Tomur’s per-resource modeling and composition approach handles multi-resource contention. We fix the traffic profile to be the default in this section to isolate its impact. We choose FlowMonitor and NIDS that utilize multiple resources, and co-run each with mem-bench and regex-bench with varying contention levels. Table 3 presents the comparison. We can observe that Tomur reduces the MAPE by 44.2% and 17.1% for FlowMonitor and NIDS, respectively. To better analyze the source of accuracy gains, we zoom in on FlowMonitor and vary the regex contention level it receives in two ranges: low range (MTBR ≤ 600 matches/MB), and high range (MTBR > 600 matches/MB). Figure 7(a) depicts the distribution of the absolute percentage errors. Tomur maintains low errors as contention rises with median errors consistently below 6.0%. With low contention, SLOMO also achieves high accuracy with median error at 2.5%, because in this case multi-resource contention effectively reduces to single-resource (memory for FlowMonitor) contention. Here Tomur’s error is actually slightly higher than SLOMO, because SLOMO enjoys the same amount of training data with Tomur but concentrate on one fixed traffic profile. During high contention, SLOMO’s inability to model contention on these two resources simultaneously lead to high median errors at 24.4%.

To further evaluate the use of Tomur’s composition design based on execution pattern (§4.2), we write two synthetic NFs, NF1 and NF2, with NF1 using memory and regex, while NF2 adds the compression accelerator. Each has both a pipeline and run-to-completion version. We compare Tomur to the simple sum and min composition (recall §2.2), where they use the same per-resource models trained specifically for NF1 and

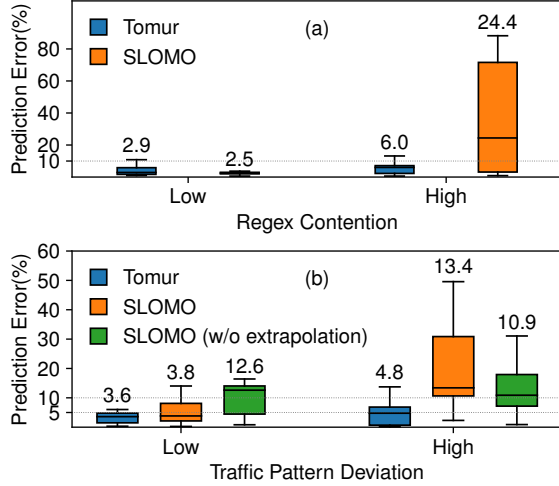


Figure 7: The distribution (box and whisker plot) of the absolute percentage errors of (a) multi-resource contention with different regex contention levels, and (b) memory-only contention with different ranges of variations in the flow count. We show the value of median error in both figures.

NF2. As shown in Table 4, Tomur attains the best accuracy across all cases and resource usage patterns, with MAPE lower than 2%. This gain essentially comes from properly modeling NF’s execution pattern to capture the end-to-end impact of multi-resource contention. Tomur is on par with min composition for pipeline NFs, which is consistent with Equation (7).

NF	Pattern	MAPE (%)		
		sum	min	Tomur
NF1	pipeline	9.8	0.7	0.7
	run-to-completion	8.7	12.4	1.3
NF2	pipeline	21.9	1.8	1.8
	run-to-completion	14.6	7.6	1.6

Table 4: Prediction error of different multi-resource composition approaches for different execution patterns.

NF	SLOMO			Tomur		
	MAPE (%)	$\pm 5\%$ Acc.(%)	$\pm 10\%$ Acc.(%)	MAPE (%)	$\pm 5\%$ Acc.(%)	$\pm 10\%$ Acc.(%)
NIDS	2.5	90.0	100.0	1.1	98.0	100.0
FlowClassifier	10.4	52.0	66.0	2.9	80.0	100.0
NAT	9.5	28.0	64.0	3.1	82.0	96.0
FlowTracker	4.0	70.0	92.0	3.5	74.0	96.0
FlowStats	9.5	44.0	66.0	4.7	72.0	92.0
FlowMonitor	11.9	20.0	44.0	4.8	62.0	88.0
IPTunnel	88.0	24.0	52.0	5.6	80.0	94.0

Table 5: Prediction accuracy of SLOMO and Tomur when target NF runs under memory-only contention and dynamic traffic profiles.

7.4 Deep-Dive: Traffic Attributes

We now move to examine Tomur’s design on traffic-aware modeling. We choose traffic-sensitive NFs and co-run each

with mem-bench on a single BF-2. Since SLOMO only considers memory contention, we set a fixed contention level in memory, exclude other resource contention, and generate 100 traffic profiles by randomly changing number of flows, packet size, and MTBR when applicable for each NF. Table 5 shows the results aggregated from all profiles. Again Tomur attains superior accuracy over SLOMO across the board, with over 90% in $\pm 10\%$ Acc. and $< 5\%$ MAPE for most NFs.

We then zoom into one particular attribute, flow count, which SLOMO also specifically models. We vary the flow count between training and testing across two ranges: low range where it changes by at most 20%, and high range ($> 20\%$). Figure 7(b) displays the distribution of absolute percentage error in this case. Tomur maintains low errors consistently, with a median at 4.7%, highlighting the benefits of our traffic-aware modeling (§5). Under low-range variations, SLOMO exhibits high accuracy with sensitivity extrapolation [42]. However, as traffic profiles undergo more significant changes, SLOMO suffers from high prediction errors, with 13.4% at the median. This is consistent with [42]: the extrapolation only works when the NF’s sensitivity profile in training has enough overlap with that under testing traffic [42], which corresponds to low range profiles here.

7.5 Tomur Use Cases

We now illustrate Tomur’s practical benefits through two use cases: (1) It enables contention-aware scheduling of NFs to improve resource utilization; (2) it facilitates performance diagnosis for NFs with dynamic traffic.

7.5.1 Contention-Aware Scheduling

We consider the scenario in which the operator places the NFs as they arrive to a group of SmartNICs to maximize resource utilization (*i.e.*, minimize SmartNICs used) while maintaining their SLAs. SLA here is defined as the maximum allowed throughput drop relative to the baseline when the NF runs solo. Given that the offline version of this problem is NP-complete bin-packing [27, 58], we follow previous works [42, 56, 61] and consider online heuristics that deploy the NFs one by one. Specifically, we compare the following strategies: (1) Monopolization, which forbids co-location of NFs; (2) Greedy, which places an NF onto the SmartNIC with most available resources [41, 53]; (3) Contention-aware, which first predicts the performance of all NFs on a SmartNIC if the current NF gets deployed onto this SmartNIC, and then deploys the NF onto the SmartNIC if no SLA violation is predicted. Both Tomur and SLOMO can provide such contention-aware predictions. A new SmartNIC is added to the cluster when there is no feasible placement.

Table 6 compares the above strategies over 100 random sequences of 500 NF arrivals each. Each NF is assigned the default traffic profile, and its SLA is set to 5-20% throughput drop. We examine resource wastage, *i.e.*, how many additional NICs are used against the optimal plan found by exhaustive

Approach	Resource Wastage (%)	SLA Violations (%)
Monopolization	196.3	0
Greedy	19.0	16.5
SLOMO	-21.8	24.4
Tomur	0.5	1.9

Table 6: Tomur’s usecase in contention-aware scheduling comparing to other baseline strategies. SLOMO’s negative resource overhead stems from erroneous placements compared to the optimal deployment.

NF	Correctness (%)	
	SLOMO	Tomur
Flowstats	100.0	100.0
FlowMonitor	38.7	100.0
IPComp Gateway	29.3	100.0

Table 7: Percentage of correct identifications of performance bottleneck using SLOMO and Tomur.

search, and the corresponding SLA violations. We observe that Tomur minimizes resource wastage to merely 0.5% and reduces SLA violations by 88.5% and 92.2% over Greedy and SLOMO on average. The near-optimal performance of Tomur illustrates its potential in coordinating NF scheduling in a real-world scenario.

7.5.2 Performance Diagnosis

In practice, performance diagnosis has important values as it allows programmers to systematically explore the design spaces, identify performance bottlenecks and optimization opportunities, and even provide early-stage insights/guidances on next-generation SmartNIC [42, 45]. Here we show another usecase of Tomur in diagnosing performance bottlenecks in NFs with dynamic traffic, when the bottleneck may shift across resources.

As Table 7 shows we deploy FlowStats, FlowMonitor, and IPComp Gateway that all use regex accelerator. We co-run each of them with mem-bench and regex-bench and adjust the MTBR from 0 to 1100 matches/MB while keeping memory contention levels unchanged, and manually analyze the actual its performance bottleneck using the hotspot analysis function of perf-tools [19]. This is the ground truth. We then calculate the percentage of correct identification of bottleneck using our prediction models. We can see Tomur accurately identifies bottleneck for all three NFs with its multi-resource performance modeling, while SLOMO only works for FlowStats, as it is always bottlenecked on memory. FlowMonitor and IPComp Gateway’s bottleneck actually shifts with traffic. For example, we observe that FlowMonitor’s bottleneck is memory with MTBR at 80 matches/MB, but changes to regex with MTBR at 1000 matches/MB (default traffic profile). Thus this usecase demonstrates Tomur’s capability in pinpointing NF bottlenecks with dynamic traffic.

NF	Full		Random		Adaptive	
	P.C.: 3200×		P.C.: 1×		P.C.: 1×	
	MAPE (%)	±10% Acc.(%)	MAPE (%)	±10% Acc.(%)	MAPE (%)	±10% Acc.(%)
FlowClassifier	2.3	100.0	14.4	28.0	2.9	100.0
NAT	2.9	98.0	9.6	62.0	3.1	96.0
FlowTracker	3.4	96.0	38.9	0.0	3.4	86.0
FlowMonitor	4.5	86.0	12.3	42.0	4.8	88.0
FlowStats	5.3	90.0	9.8	68.0	4.9	90.0
IPTunnel	5.3	98.0	8.5	82.0	5.9	96.0

Table 8: Profiling cost and model accuracy using full, random and Tomur’s adaptive profiling. P.C. refers to profiling cost.

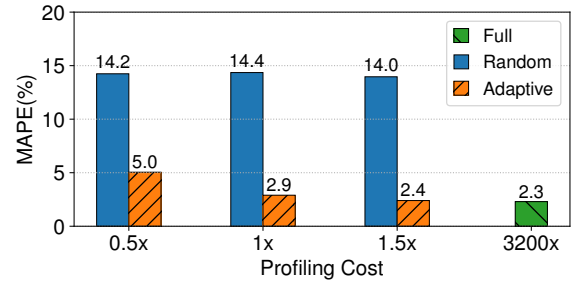


Figure 8: Prediction error on FlowClassifier using full, random and Tomur’s adaptive profiling. We change the profiling quota of random and adaptive profiling to 0.5× and 1.5× of that used in Table 8.

7.6 Offline Profiling

Lastly we examine the adaptive profiling design of Tomur.

Adaptive profiling. To evaluate Tomur’s adaptive profiling, we select traffic-sensitive NFs from Table 1, and train them using three different approaches — full profiling, random profiling, and adaptive profiling (§5.2). For random profiling and Tomur’s adaptive profiling, we set the same number of training data points (*a.k.a.* profiling quota) to ensure a fair comparison. For full profiling, we use 80% of the profiled data for training, and the remaining 20% for testing. Profiling cost is represented by the number of training data samples normalized against adaptive/random profiling’s quota. We observe from Table 8 that Tomur’s adaptive profiling offers comparable accuracy to full profiling which uses 3200× more data. Compared to random, adaptive profiling significantly enhances accuracy within the same profiling quota. Notably, it achieves a maximum 35.5% MAPE reduction on FlowTracker and a 72% improvement in ±10% Acc. on FlowClassifier over random. We further show the benefit of adaptive profiling using FlowClassifier as an example in Figure 8. We adopt same setting as Table 8 but change the profiling quota to 0.5× and 1.5×. Figure 8 reveals that by increasing current profiling quota by 50% (still ~2100× less than the profiling cost of full profiling), adaptive profiling achieve similar error compared to full profiling, at 2.4% and 2.3%, respectively, while random profiling does not exhibit accuracy improvement since performance-significant ranges of traffic attribute

NF	SLOMO			Tomur		
	MAPE (%)	$\pm 5\%$ Acc.(%)	$\pm 10\%$ Acc.(%)	MAPE (%)	$\pm 5\%$ Acc.(%)	$\pm 10\%$ Acc.(%)
Firewall	18.4	58.7	64.7	0.9	100.0	100.0

Table 9: Prediction accuracy of SLOMO and Tomur when target NF runs under memory-only contention and dynamic traffic profiles on Pensando SmartNIC.

is still not covered in the training data.

Time cost of profiling. As discussed in §6, Tomur requires offline profiling for each NF to build per-resource models and identify execution pattern. This process primarily involves collection of: (1) the contention level of synthetic benchmark NFs, and (2) contention level and sensitivity profiles of target NFs. Across our experiments, we find that on average 1.6 hours and 0.5 hour are spent on profiling the contention level of synthetic benchmark NFs (mem-bench, etc.) and the contention level and sensitivity profiles of an NF, respectively. These time investments are acceptable since profiling is a one-time effort.

8 Discussion

Can Tomur be generalized to other SmartNICs? Tomur can be generalized to other SoC SmartNICs due to the similar architecture of their hardware accelerators and memory subsystem. To quickly validate such generalizability, we collect data and train performance models of a Firewall NF [24] running on an AMD Pensando SmartNIC [13]. The NF conducts a flow walk on hardware flow table and updates entry metadata upon matching against flows in the input traffic, thus requires memory and regex accelerator. As shown in Table 9, the average prediction error of Tomur is 0.9%, which is 17.5% lower compared to that of SLOMO. Such preliminary result reflects that applying Tomur to other SoC SmartNICs is feasible. However, for SmartNICs whose architecture significantly deviates from SoC SmartNICs, *e.g.*, on-path SmartNICs, we require more investigations on the contention behavior of their specialized hardware resources [30, 38]. We leave this as future work.

What if the configuration of an NF changes? It is possible that an NF’s configuration is adjusted for various reasons. Such changes can cause performance characteristics to change, making the existing model inaccurate. To make Tomur “configuration-aware”, one may adopt a similar approach of traffic attributes, *i.e.*, extracting “configuration attributes” for an NF and integrating it into the per-resource models. We leave this as future work.

9 Related Work

NF performance modeling. There have been extensive efforts on modeling NF performance. We compare Tomur with past frameworks in Table 10. Tomur is, to our knowledge, the first contention-aware framework that explicitly models

Framework	Contention-aware	Multi-resource	Traffic-aware	Sourcecode-agnostic
Clara [49]	×	✓	✓	×
LogNIC [32]	×	✓	✓	✓
BubbleUp [44]	✓	×	×	✓
SLOMO [42]	✓	×	×	✓
Tomur	✓	✓	✓	✓

Table 10: NF performance prediction frameworks. “Sourcecode-agnostic” means the framework does not require NF’s source code. SLOMO only considers 20% variation in flow counts.

multi-resource contention and traffic attributes.

Isolation. Resource isolation techniques have been explored to provide performance guarantees of co-running applications. For example, FairNIC [31] proposes isolation solutions for SmartNIC accelerators. PARTIES [26] and ResQ [56] leverages off-the-shelf isolation techniques, *e.g.*, Intel CAT [16] to enable QoS-aware resource partitioning. PicNIC [35] enables isolation in the network virtualization stack shared by tenant VMs. Netbricks [48] leverages its safe runtime to provide software-level isolation on servers. However, these efforts are either inapplicable to SmartNICs, or provide only partial isolation, or require substantial rewriting of NFs.

SmartNIC-accelerated NFV. NFV platforms have been leveraging SmartNICs to improve energy efficiency and enable host resource-saving [34, 36, 40, 41, 51, 53]. For example, E3 [41] builds a SmartNIC-accelerated microservice execution platform with high energy efficiency. Meili [53] provides a novel framework to achieve high resource efficiency and scalable NF performance across the SmartNIC cluster. Tomur is complementary to them as it can assist operators to make better runtime decisions, thus improving resource utilization and reducing SLA violations.

10 Conclusion

Prior contention-aware performance prediction frameworks fail to accurately predict the performance of on-NIC NFs due to multi-resource contention and changing traffic profiles. We systematically analyze multi-resource contention characteristics on SmartNIC as well as the impact of traffic attributes on performance of on-NIC NFs. Our insights enable the design of Tomur, an NF performance prediction framework applicable to multi-resource contention and changing traffic attributes. Tomur features per-resource contention modeling and traffic-aware argumentation to reduce multi-resource contention to single-resource contentions and integrate traffic-aware knowledge into per-resource models. Evaluations on common on-NIC NFs demonstrate that Tomur achieves accurate performance predictions, with 3.7% prediction error and 78.8% accuracy improvement on average compared to prior works, 88.5% higher resource utilization and 92.2% less SLA violations in NF placement, and 100% accurate performance bottleneck diagnosis.

References

- [1] RDMA Active Queue Pair Operations. <https://docs.nvidia.com/networking/display/rdmaawareprogrammingv17/rdma+active+queue+pair+operations>.
- [2] The (de)compression accelerator on NVIDIA BlueField-2 SmartNIC. <https://docs.nvidia.com/networking/display/BlueFieldDPUOSLatest/Compression+Acceleration>.
- [3] The RegEx accelerator on NVIDIA BlueField-2 SmartNIC. <https://docs.nvidia.com/networking/display/BlueFieldDPUOSLatest/RegEx+Acceleration>.
- [4] NVIDIA NICs Performance Report with DPDK 23.07. https://fast.dpdk.org/doc/perf/DPDK_23_07_NVIDIA_NIC_performance_report.pdf, 2021.
- [5] Performance Tuning for Mellanox Aadpters. <https://enterprise-support.nvidia.com/s/article/performance-tuning-for-mellanox-adapters>, 2022.
- [6] DOCA Documentation v1.5.0 LTS. <https://docs.nvidia.com/doca/archive/doca-v1.5.0/>, 2023.
- [7] Dpdk. <https://www.dpdk.org>, 2023.
- [8] L7-Filter. <https://l7-filter.sourceforge.net/>, 2023.
- [9] mlx-regex. <https://github.com/Mellanox/mlx-regex>, 2023.
- [10] NVIDIA Bluefield-2 DPU. <https://resources.nvidia.com/en-us-accelerated-networking-resource-library/bluefield-2-dpu-datasheet>, 2023.
- [11] NVIDIA Bluefield-3 DPU. <https://www.nvidia.com/content/dam/en-zz/Solutions/Data-Center/documents/datasheet-nvidia-bluefield-3-dpu.pdf>, 2023.
- [12] Nvidia Developer Forums. <https://forums.developer.nvidia.com/t/performance-counters-for-accelerators/247086>, 2023.
- [13] Pensando Distributed Services Architecture SmartNIC. <https://www.servethehome.com/pensando-distributed-services-architecture-smartnic/>, 2023.
- [14] Anonymous code repository. <https://anonymous.4open.science/r/Tomur-1EF5/>, 2024.
- [15] EXREX. <https://github.com/asciimoo/exrex>, 2024.
- [16] Intel CAT. <https://github.com/intel/intel-cmt-cat>, 2024.
- [17] Internet protocol (ip) pipeline application. https://doc.dpdk.org/guides20.11/sample_app_ug/ip_pipeline.html, 2024.
- [18] Memory Bandwidth Benchmark. <https://github.com/raas/mbw>, 2024.
- [19] Perf-tools. <https://github.com/brendangregg/perf-tools>, 2024.
- [20] Rxpbench. <https://docs.nvidia.com/doca/archive/doca-v1.5.0/rxpbench/index.html>, 2024.
- [21] Scikit-learn. <https://scikit-learn.org/stable/index.html>, 2024.
- [22] Stress-ng. <https://github.com/ColinIanKing/stress-ng>, 2024.
- [23] The Pktgen Application. <https://pktgen-dpdk.readthedocs.io/en/latest/>, 2024.
- [24] Deepak Bansal, Gerald DeGrace, Rishabh Tewari, Michal Zygmunt, James Grantham, Silvano Gai, Mario Baldi, Krishna Doddapaneni, Arun Selvarajan, Arunkumar Arumugam, Balakrishnan Raman, Avijit Gupta, Sachin Jain, Deven Jagasia, Evan Langlais, Pranjali Srivastava, Rishiraj Hazarika, Neeraj Motwani, Soumya Tiwari, Stewart Grant, Ranveer Chandra, and Srikanth Kandula. Disaggregating Stateful Network Functions. In *Proc. USENIX NSDI*, 2023.
- [25] Quan Chen, Hailong Yang, Minyi Guo, Ram Srivatsa Kannan, Jason Mars, and Lingjia Tang. Prophet: Precise qos prediction on non-preemptive accelerators to improve utilization in warehouse-scale computers. In *Proc. ACM ASPLOS*, 2017.
- [26] Shuang Chen, Christina Delimitrou, and José F. Martínez. Parties: Qos-aware resource partitioning for multiple interactive services. In *Proc. ACM ASPLOS*, 2019.
- [27] E. G. Coffman, M. R. Garey, and D. S. Johnson. Approximation algorithms for bin packing: a survey. page 46–93, 1996.
- [28] Mihai Dobrescu, Katerina Argyraki, and Sylvia Ratnasamy. Toward predictable performance in software packet-processing platforms. In *Proc. USENIX NSDI*, 2012.

- [29] Kohler Eddie, Morris Robert, Chen Benjie, Jannotti John, and Kaashoek M. Frans. The click modular router. *ACM Transactions on Computer Systems*, 18(3):263–297, 2000.
- [30] Daniel Firestone, Andrew Putnam, Sambhrama Mundkur, Derek Chiou, Alireza Dabagh, Mike Andrewartha, Hari Angepat, Vivek Bhanu, Adrian Caulfield, Eric Chung, Harish Kumar Chandrappa, Somesh Chaturmohita, Matt Humphrey, Jack Lavier, Norman Lam, Fengfen Liu, Kalin Ovtcharov, Jitu Padhye, Gautham Popuri, Shachar Raindel, Tejas Sapre, Mark Shaw, Gabriel Silva, Madhan Sivakumar, Nisheeth Srivastava, Anshuman Verma, Qasim Zuhair, Deepak Bansal, Doug Burger, Kushagra Vaid, David A. Maltz, and Albert Greenberg. Azure Accelerated Networking: SmartNICs in the public cloud. In *Proc. USENIX NSDI*, 2018.
- [31] Stewart Grant, Anil Yelam, Maxwell Bland, and Alex C. Snoeren. SmartNIC Performance Isolation with FairNIC: Programmable Networking for the Cloud. In *Proc. ACM SIGCOMM*, 2020.
- [32] Zerui Guo, Jia-Jen Lin, Daehyeok Kim, Michael Swift, Aditya Akella, Ming Liu, and Yuebin Bai. Lognic: A high-level performance model for smartnics. In *Proc. IEEE/ACM MICRO*, 2023.
- [33] Anuj Kalia, Michael Kaminsky, and David G. Anderson. Design Guidelines for High Performance RDMA Systems. In *Proc. USENIX ATC*, 2016.
- [34] Daehyeok Kim, Vyas Sekar, and Srinivasan Seshan. ExoPlane: An Operating System for On-Rack Switch Resource Augmentation. In *Proc. USENIX NSDI*, 2023.
- [35] Praveen Kumar, Nandita Dukkupati, Nathan Lewis, Yi Cui, Yaogong Wang, Chonggang Li, Valas Valancius, Jake Adriaens, Steve Gribble, Nate Foster, and Amin Vahdat. Picnic: Predictable virtualized nic. In *Proc. ACM SIGCOMM*, 2019.
- [36] Yanfang Le, Hyunseok Chang, Sarit Mukherjee, Limin Wang, Aditya Akella, Michael M. Swift, and T. V. Lakshman. UNO: Uniflying host and Smart NIC offload for flexible packet processing. In *Proc. ACM SoCC*, 2017.
- [37] Bojie Li, Kun Tan, Layong (Larry) Luo, Yanqing Peng, Renqian Luo, Ningyi Xu, Yongqiang Xiong, Peng Cheng, and Enhong Chen. ClickNP: Highly Flexible and High Performance Network Processing with Reconfigurable Hardware. In *Proc. ACM SIGCOMM*, 2016.
- [38] Jiaxin Lin, Kiran Patel, Brent E. Stephens, Anirudh Sivaraman, and Aditya Akella. PANIC: A High-Performance programmable NIC for multi-tenant networks. In *Proc. USENIX OSDI*, 2020.
- [39] Jianshen Liu, Carlos Maltzahn, Craig D. Ulmer, and Matthew Leon Curry. Performance Characteristics of the BlueField-2 SmartNIC. In *Arxiv*, 2021.
- [40] Ming Liu, Tianyi Cui, Henry Schuh, Arvind Krishnamurthy, Simon Peter, and Karan Gupta. Offloading Distributed Applications onto SmartNICs Using IPipe. In *Proc. ACM SIGCOMM*, 2019.
- [41] Ming Liu, Simon Peter, Arvind Krishnamurthy, and Phitchaya Mangpo Phothilimthana. E3: Energy-Efficient Microservices on SmartNIC-Accelerated Servers. In *Proc. USENIX ATC*, 2019.
- [42] Antonis Manousis, Rahul Anand Sharma, Vyas Sekar, and Justine Sherry. Contention-aware performance prediction for virtualized network functions. In *Proc. ACM SIGCOMM*, 2020.
- [43] Jason Mars, Lingjia Tang, and Robert Hundt. Heterogeneity in “homogeneous” warehouse-scale computers: A performance opportunity. *IEEE Computer Architecture Letters*, 10(2):29–32, 2011.
- [44] Jason Mars, Lingjia Tang, Robert Hundt, Kevin Skadron, and Mary Lou Soffa. Bubble-up: Increasing utilization in modern warehouse scale computers via sensible colocations. In *Proc. IEEE/ACM MICRO*, 2011.
- [45] Sebastiano Miano, Alireza Sanaee, Fulvio Risso, Gábor Rétvári, and Gianni Antichi. Domain specific run time optimization for software data planes. In *Proc. ACM ASPLOS*, 2022.
- [46] Amirhossein Mirhosseini and Thomas F. Wenisch. The queuing-first approach for tail management of interactive services. *IEEE Micro*, 39(4):55–64, 2019.
- [47] Katsikas Georgios P., Barbette Tom, Kostić Dejan, Steinert Rebecca, and Maguire Gerald Q. Metron: Nfv service chains at the true speed of the underlying hardware. In *Proc. USENIX NSDI*, 2018.
- [48] Aurojit Panda, Sangjin Han, Keon Jang, Melvin Walls, Sylvia Ratnasamy, and Scott Shenker. NetBricks: Taking the v out of NFV. In *Proc. USENIX OSDI*, 2016.
- [49] Yiming Qiu, Jiarong Xing, Kuo-Feng Hsu, Qiao Kang, Ming Liu, Srinivas Narayana, and Ang Chen. Automated SmartNIC Offloading Insights for Network Functions. In *Proc. ACM SOSP*, 2021.
- [50] Robert R. Schaller. Moore’s law: Past, present, and future. *IEEE Spectr.*, 34(6):52–59, 1997.
- [51] Yizhou Shan, Will Lin, Ryan Kosta, Arvind Krishnamurthy, and Yiyang Zhang. Disaggregating and Consolidating Network Functionalities with SuperNIC. In *Arxiv*, 2022.

- [52] Rajath Shashidhara, Tim Stamler, Antoine Kaufmann, and Simon Peter. FlexTOE: Flexible TCP Offload with Fine-Grained Parallelism. In *Proc. USENIX NSDI*, 2022.
- [53] Qiang Su, Shaofeng Wu, Zhixiong Niu, Ran Shu, Peng Cheng, Yongqiang Xiong, Chun Jason Xue, Zaoxing Liu, and Hong Xu. Meili: Enabling smartnic as a service in the cloud. In *Arxiv*, 2024.
- [54] Chen Sun, Jun Bi, Zhilong Zheng, Heng Yu, and Hongxin Hu. NFP: Enabling network function parallelism in NFV. In *Proc. ACM SIGCOMM*, 2017.
- [55] Naru Sundar, Brad Burres, Yadong Li, Dave Minturn, Brian Johnson, and Nupur Jain. An In-depth Look at the Intel IPU E2000. In *Proc. IEEE ISSCC*, 2023.
- [56] Amin Tootoonchian, Aurojit Panda, Chang Lan, Melvin Walls, Katerina Argyraki, Sylvia Ratnasamy, and Scott Shenker. ResQ: Enabling SLOs in network function virtualization. In *Proc. USENIX NSDI*, 2018.
- [57] Xingda Wei, Rongxin Cheng, Yuhan Yang, Rong Chen, and Haibo Chen. Characterizing off-path SmartNIC for accelerating distributed systems. In *Proc. USENIX OSDI*, 2023.
- [58] Andrew Chi-Chih Yao. New algorithms for bin packing. *Journal of the ACM*, 27(2):207–227, 1980.
- [59] Li Lyna Zhang, Shihao Han, Jianyu Wei, Ningxin Zheng, Ting Cao, Yuqing Yang, and Yunxin Liu. nn-meter: Towards accurate latency prediction of deep-learning model inference on diverse edge devices. In *Proc. ACM MobiSys*, 2021.
- [60] Wei Zhang, Guyue Liu, Wenhui Zhang, Neel Shah, Phillip Lopreiato, Gregoire Todeschi, K.K. Ramakrishnan, and Timothy Wood. OpenNetVM: A Platform for High Performance Network Service Chains. In *Proc. ACM HotMiddlebox*, 2016.
- [61] Zhilong Zheng, Jun Bi, Heng Yu, Haiping Wang, Chen Sun, Hongxin Hu, and Jianping Wu. Octans: Optimal placement of service function chains in many-core systems. In *Proc. IEEE INFOCOM*, 2019.

Appendices

A Accuracy of Single-Resource Models

We validate the accuracy of single-resource performance model for memory subsystem contention (SLOMO) and regex accelerator contention (§4.1.1), and present results in Table 11 and 12, respectively.

NF	MAPE (%)	±5% Acc.(%)	±10% Acc.(%)
IPRouter	1.8	90.0	100.0
FlowStats	1.2	100.0	100.0
NAT	2.5	88.0	96.0
IP Tunnel	0.6	98.0	100.0
FlowMonitor	0.9	98.0	100.0
NIDs	0.7	100.0	100.0
FlowTracker	1.6	96.0	100.0
ACL	2.2	100.0	100.0
FlowClassifier	1.1	94.0	100.0

Table 11: End-to-end prediction error of SLOMO when target NF runs under memory-only contention and fixed traffic profile. SLOMO attains high accuracy regarding memory subsystem contention at fixed traffic profile.

NF	MAPE (%)	±5% Acc.(%)	±10% Acc.(%)
FlowMonitor	1.3	94.1	100.0
NIDs	1.2	100.0	100.0

Table 12: End-to-end prediction error of our regex model when target NF runs under regex-only contention and fixed traffic profile. Our regex model shows high accuracy regarding regex contention at fixed traffic profile.

B Contention in Memory Subsystem

Setup. We co-run FlowStats with mem-bench and draw NF’s throughput regarding competing working set size (WSS) at different competing cache access rate (CAR) in Figure 9. We adjust both the working set size (WSS) and cache access rate (CAR) of mem-bench to apply different types of pressure on memory subsystem.

Observation. The figure shows decreasing throughput of FlowStats with higher CAR and WSS. The performance drop is because of high cache evictions caused by the noisy neighbor’s cache access behavior. Below ~6 MB competing WSS, NF performance is mainly affected by competing WSS rather than CAR, while above this threshold, CAR becomes the key actor that affects NF performance. This observation meets the 6MB size of L3 cache on a BlueField-2 SmartNIC, and also indicates the need to model the contention in SmartNIC’s memory subsystem by considering multiple fine-grained metrics of it, *i.e.*, access rate and occupancy of last level cache.

C Formula

Based on Equation 3 and 4, the composition function F adopted in execution-pattern-based composition can be represented as follows:

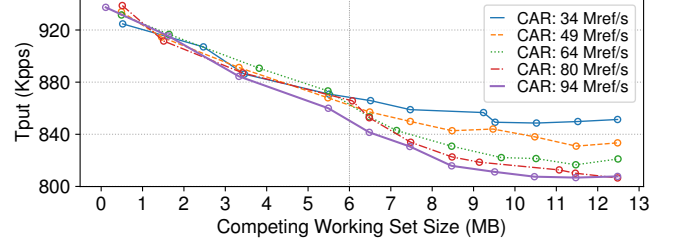


Figure 9: The throughput of Flowstats as a function of competing working set size and cache access rate. The traffic profile has 16K flows. The packet size is 1500 B.

$$F(E, T_{solo}, \Delta T_1, \dots, \Delta T_r) = \begin{cases} T_{solo} - \max(\Delta T_1, \dots, \Delta T_r), & \text{if } E = pl \\ \frac{1}{\sum_{j=1}^r \left(\frac{1}{T_{solo} - \Delta T_j} \right) - \frac{r-1}{T_{solo}}}, & \text{if } E = rtc \end{cases} \quad (7)$$

where E represents execution pattern, pl and rtc stand for pipeline and run-to-completion pattern.

D Performance Counters

We list the performance counters Tomur uses to measure contention level in memory subsystem in Table 13. These performance counters are selected according to [42].

Counter	Definition
IPC	Instructions per cycle.
IRT	Instruction retired.
L2CRD	L2 data cache read access.
L2CWR	L2 data cache write access.
MEMRD	Data memory read access.
MEMWR	Data memory write access.
WSS	Working set size.

Table 13: Performance counters for training the per-resource model of memory subsystem.

E Validation of Queue-Based Model

Equation 2 explicitly models NF’s performance regarding regex contention, but how it is aligned with experiment results in Figure 4 is unclear. Therefore, we show that two properties of Figure 4 — linearity and equilibrium (recall §4.1.1), can be derived and explained using Equation 2.

Linearity. In Figure 4, we run a synthetic regex-NF (denoted as NF_1) with regex-bench, each of which construct one request queue with the regex accelerator. Suppose that we control the arrival rate of regex-bench to T_C (just as we did in Figure 4), then in each unit of time of regex accelerator, the processing of regex-bench’s request will take away $T_C t_C$ unit of time, where t_C is the average per-request processing time of regex-bench’s requests. This means that only $(1 - T_C t_C)$ unit of time is left for the processing of NF_1 . Therefore, the throughput of NF_1 (denoted as T_1) can be represented as:

$$T_1 = (1 - T_C t_C) T_{1,solo} = T_{1,solo} - \frac{T_{1,solo}}{T_{C,solo}} T_C \quad (8)$$

where $T_{1,solo}$ and $T_{c,solo}$ represent solo throughput of regex processing in NF_1 and regex-bench. Equation 8 is aligned with the linearity between NF_1 's throughput and competing throughput from regex-bench.

Equilibrium. Since both NF_1 and regex-bench only construct one queue with regex accelerator, we can calculate regex-bench's equilibrium throughput as: $T_E = \frac{1}{\frac{1}{T_{1,solo}} + \frac{1}{T_{C,solo}}}$ based on Equation 2. By assigning T_E to T_C in Equation 8, we can derive that $T_1 = (1 - \frac{T_E}{T_{C,solo}})T_{1,solo} = T_E$, indicating that the regex-NF and regex-bench achieve same throughput of $T_1 = \frac{1}{\frac{1}{T_{1,solo}} + \frac{1}{T_{C,solo}}}$. This is also aligned with the observation that an equilibrium will be achieved for NFs sharing the regex accelerator.

F Detailed Workflow of Tomur

F.1 General Workflow

To apply Tomur on an NF (NF_i), a general workflow can be split to (1) offline profiling and training, (2) online prediction.

Offline profiling and training. Tomur first collects contention level of NF_i and synthetic competitors, and the throughput of NF_i when co-running synthetic competitors with NF_i under different traffic profiles. In the training phase, we train per-resource models of NF_i using the (contention level, traffic attribute, throughput) tuple.

Online profiling. We use contention level of competitors (profiled) and traffic attributes of current traffic profile (provided) as model input to obtain . Then we compose these partial predictions based on execution pattern of NF_i (provided) to obtain end-to-end throughput predictions.

We show details of offline profiling and training in appendix §F.2 and online prediction in appendix §F.3.

F.2 Offline Profiling and Training

Tomur collects necessary profiles of synthetic competitors and NF_i . For synthetic competitors, their contention levels on shared resources are collected. For NF_i , Tomur collects its contention level on shared resources and its throughput under different levels of single-resource contention and traffic profiles.

Contention level of synthetic competitor. We measure the contention level that synthetic competitors applies on their corresponding resource. In our current design, we consider the contention in regex accelerator and memory subsystem. Therefore, for each configuration (denoted as c) of synthetic competitor, we collect contention level of regex-bench ($C_{R,c}$) and mem-bench ($C_{M,c}$).

For regex-bench, we run regex-bench independently on SmartNIC. We adjust per-request processing time ($t_{R,c}$) of regex-bench by changing MTBR of input traffic profile. The number of request queues of regex-bench is fixed to 1. Then the contention level of regex-bench is represented as $C_{R,c} = (1, t_{R,c})$ for each configuration.

For mem-bench, we run mem-bench independently on SmartNIC. We adjust contention level of mem-bench by changing the memory access pattern, memory access speed and working set size of it. For each configuration, we collect runtime performance counters shown in appendix §D (denoted as $pc_{1,c}, \dots, pc_{k,c}$) of mem-bench. Therefore, the contention level of mem-bench is represented as $C_{R,c} = (pc_{1,c}, \dots, pc_{k,c})$.

Note that the profiling of synthetic competitors is a one-time effort for all NFs, meaning that any NF can reuse the profiling data of synthetic competitors to train its models.

Contention level of NF_i . We measure the contention level that NF_i applies on R types of shared resources under different traffic profiles (P). A traffic profile P can be denoted as a vector of traffic attributes (p_1, \dots, p_l). In our current design, we measure the contention NF_i applies on regex accelerator ($C_{i,r,P}$) and memory subsystem ($C_{i,m,P}$), respectively.

To measure $C_{i,r}$, we co-run NF_i with regex-bench. Since the per-request processing time of regex-bench has already been profiled, we calculate the number of queues (n_i) and per-request processing time ($t_{i,P}$) of NF_i using Equation 2. Therefore, the contention level of NF_i on regex accelerator can be represented as $C_{i,r,P} = (n_i, t_{i,P})$

To measure $C_{i,m}$, we run NF_i independently on SmartNIC. We measure contention levels of NF_i under a series of traffic profiles by collecting runtime performance counters $pc_{1,P}, \dots, pc_{k,P}$ of NF_i . Therefore, the contention level of NF_i on memory subsystem can be represented as $C_{i,c,P} = (pc_{1,P}, \dots, pc_{k,P})$. We also measure the solo throughput ($T_{i,solo}$) of NF_i by the way.

Training data of NF_i . We collect training data of NF_i for memory subsystem model using adaptive profiling algorithm. The algorithm co-runs (1) mem-bench using different configurations (c) with (2) NF_i using different traffic profile (P), and measure the interfered throughput ($T_{i,c,P}$) of NF_i . Note that the dimension of P is pruned by adaptive profiling for each NF's memory model.

Due to the explicit form of NF_i 's regex model, collection of a small amount of data (< 10) is enough. Similarly, we co-run (1) regex-bench using different configurations (c) and, (2) NF_i using different traffic profile (P), and measure the interfered throughput ($T_{i,c,P}$) of NF_i . Note that we only consider the change of MTBR in P for regex model.

Specifically, each entry of training data for NF_i 's per-resource models can be represented as:

1. Memory subsystem model: $((C_{M,c}, P), T_{i,c,P})$
2. Regex model: $((C_{R,c}, P), T_{i,c,P})$

Model training. We leverage the profiled data to train per-resource models of NF_i . We denote the memory subsystem model and regex model of NF_i as $M_{i,m}$ and $M_{i,r}$ respectively. To train $M_{i,m}$, we use $(C_{M,c}, P)$ as input feature and $T_{i,c,P}$ as label. To train $M_{i,r}$, we use Equation 2 to calculate number of request queues and per-request processing time of NF_i . According to Equation 6, we use linear regression to correlate

per-request processing time of NF_i with MTBR (as in P).

F.3 Online Prediction

Suppose that NF_i is co-located with a group of competitors $\mathcal{A} = \{NF_1, \dots, NF_n\}$. To predict the throughput of NF_i , Tomur requires the following inputs:

- (1) P : traffic profile of NF_i (provided).
- (2) E : execution pattern of NF_i (provided).
- (3) $T_{solo,P}$: solo throughput of NF_i using traffic profile P (profiled).
- (4) C_j , $\forall j$ s.t. $NF_j \in \mathcal{A}$: contention level of each competitor on memory subsystem $C_{j,m}$ and $C_{j,r}$ (profiled).

We use (1) and (4) as input to $M_{i,m}$ and $M_{i,r}$ to predict throughput drop of NF_i under traffic profile P caused by contention in memory subsystem ($\Delta T_{i,m}$) and regex accelerator ($\Delta T_{i,r}$) respectively. Then we use $\Delta T_{i,m}$, $\Delta T_{i,r}$, (2) and (3) as input to our composition formula (Equation 7) to obtain end-to-end throughput prediction of NF_i .